AMERICAN SCIENTIFIC PUBLISHERS

Journal of Nanofluids
Vol. 9, pp. 362–374, 2020
(www.aspbs.com/jon)

ARTICLE

Thermo-Solutal Convection of a Nanofluid Utilizing Fourier's-Type Compass Conditions

J. C. Umavathi[1,*] and Ali J. Chamkha[2]

[1]*Department of Mathematics, Gulbarga University, Gulbarga-585 106, Karnataka, India*
[2]*Faculty of Engineering, Kuwait College of Science and Technology, Doha District, 35004, Kuwait*

Nanotechnology has infiltrated into duct design in parallel with many other fields of mechanical, medical and energy engineering. Motivated by the excellent potential of nanofluids, a subset of materials engineered at the nanoscale, in the present work, a new mathematical model is developed for natural convection in a vertical duct containing nanofluid. Numerical scrutiny for the double-diffusive free and forced convection within a duct encumbered with nanofluid is performed. Buongiorno's model is deployed to define the nanofluid. Robin boundary conditions are used to define the surface boundary conditions. Thermal and concentration equations envisage the viscous, Brownian motion, thermosphores of the nanofluid, Soret and Dufour effects. Using the Boussinesq approximation the solutal buoyancy effect as a result of gradients in concentration are incorporated. The conservation equations which are nonlinear are numerically estimated using fourth order Runge-Kutta methodology and analytically ratifying regular perturbation scheme. The mass, heat, nanoparticle concentration and species concentration fields on eight dimensionless physical parameters such as thermal and mass Grashof numbers, Brownian motion parameter, thermal parameter, Prandtl number, Eckert number, Schmidt parameter, and Soret parameter are calculated. The impact of these parameters are outlined pictorially. The velocity and temperature fields are boosted with the thermal Grashof number. The Soret and the Schemidt parameters reduces the nanoparticle volume fraction but it heightens the momentum, temperature and concentration. At the cold wall thermal and concentration Grashof numbers reduces the Nusselt values but they increase the Nusselt values at the hot wall. The reversal consequence was attained at the hot plate. The perturbation and Runge-Kutta solutions are equal in the nonappearance of Prandtl number. The (E. Zanchini, *Int. J. Heat Mass Transfer* 41, 3949 (1998)). results are restored for the regular fluid. The heat transfer rate is high for nanofluid when matched with regular fluid.

KEYWORDS: Nanofuild, Double-Diffusion, Convective Boundary Conditions, Runge-Kutta Shooting Technique.

1. INTRODUCTION

Nanofluid is an enhanced type of fluid accomplished with a two phase mixture prepared by diffusing nanometer sized particles in conventional fluids. The nanometer sized materials could be nanoparticles, nanowires, nanorods, nanotubes or nanofibers while the base fluids could be water, oils, biofluids, lubricants, organic liquid (refrigerants, glycols, ethylene) and routine liquids. The combination of any of the distinct materials and a regular fluid yields a Nanofluid.

The initial success of nanofluids in aerospace and automotive applications (radiator and jet engine thermal management) have stimulated intense activity in the research community exploring the deployment of these nanomaterials in other branches of science.[1]

Materials which include alumina, silica, titania metal oxides, oxide ceramics, gold, copper are chemically stable metals when utilized as nanoparticles. Xie et al.[2] analyzed nanofluids acquired amplification of thermo physical properties namely viscosity, conductivity of heat, and advective coefficient of heat transfer related to carrier fluids for instance water or oil. Choi[3] pioneered the proposition that fluids dropped with nanoparticles can be stated as nanofluids and concluded that nanofluids are deployed as thermal transfer fluids because they can intensify energy transfer efficiency compared to pure liquids. Keblinski et al.,[4] Wang and Wang and Mujumdar[5], Kumar et al.[6] pioneered that nanofluids have the improved transmission of heat than the conventional fluids and the better possibilities depend upon the type, size and concentration of nanoparticles. The attribute of nanofluids is to reinforce the thermal conductivity, a phenomenon explained by Mausuda et al.[7] Also, such type phenomenon proposes the potentiality of using nanofluid in progressive nuclear plant introduced by Buongiorno and Hu[8]. The nanofluids are also pertinent in

*Author to whom correspondence should be addressed.
Email: drumavathi@rediffmail.com
Received: 23 April 2021
Accepted: 11 May 2021

nano-drug dispatch which explained by Kleinstreuer and Feng[9]. The compressive review in nanofluids was done by Buongionrno[10], who points that a adequate clarification for the unusual surge of the conductivity of heat and viscosity needs to be constructed. The Rayleigh-Benard problem was researched by Nield and Kuznetsov[11, 12]. They achieved that the thermophoresis and Brownian diffusion generate cross-diffusion and are identical with the Dufour and Soret cross diffusion which appear in binary fluid. Kim et al.[13, 14] and Savino and Paterna[15] also researched on this aspect of transport in nanofluids.

Investigation of nanoparticles Cu, Ag and Fe_3O_4on thermophoresis and viscous dissipation of MHD nanofluid over a stretching sheet in a porous regime was designed numerically by Hazarika et al.[16] They concluded that the greater nanoparticle volume fraction declines the liquid velocity, while a nondecline situation has occurred for liquid temperature. Furthermore, the velocity always overshoots for Fe_3O_4-water nanofluid, followed by Cu and Ag-water nanofluid, whereas the reverse performance was observed for the temperature profiles. A theoretical investigation for internal heat generation, suction/injection, diffusion-thermo and nano-particle volume fraction on a chemically reacting hydro-magnetic flow of Cu-water nano-fluid over a semi-infinite vertical surface was presented by Hazarika et al.[17]. It was found that by increasing porosity parameter decelerated the flow velocity for both nano-fluid and base fluid, whereas it enhanced the temperature for the radiation parameter. For the impact of free convection and diffusion-thermo, growth values of flow velocity were detected for nano-fluid (Cu) than the base fluid (water).

Recently several researchers studied about the double-diffusive convection in a porous cavity. Goyeau et al.[18] worked using Darcy-Brinkman formulation, the double-diffusion in a pervious cavity. Ahmed et al.[19] examined the effects of Darcian drag force and radiation-conduction on unsteady two-dimensional magnetohydrodynamic flow of viscous, electrically conducting and Newtonian fluid over a vertical plate adjacent to a Darcian regime in presence of thermal radiation and transversal magnetic field. It was found that, with a rise in the Darcian drag force, flow velocity and temperature were reduced, but increased for all times. Both average and local skin frictions were reduced considerably with an increase in Darcian drag force, but reversed behavior was observed for the local Nusselt number. Analytical solutions were determined by Ahmed et al.[20] on the oscillatory hydromagnetic flow of a viscous, incompressible, electrically-conducting, non-Newtonian fluid in an inclined, rotating channel with non-conducting walls, incorporating couple stress effects. They claimed that the magnetic field serves to inhibit primary flow in the channel; secondary back flow was however initially enhanced with increasing magnetic field effects, but closer to the upper plate was impeded. Analytical and numerical solutions of a non-linear MHD flow with heat and mass transfer characteristics of an incompressible, viscous, electrically conducting and Boussinesq's fluid over a vertical oscillating plate embedded in a Darcian porous medium in the presence of thermal radiation effect was presented by Ahmed et al.[21]. An increase in porosity parameter depressed the fluid velocities and shear stress in the regime. Also they found that, when the conduction-radiation was increased, the fluid velocity and the temperature profiles were declined.

Karimi-Fard et al.[22] and Nithiarasu et al.[23] worked on the non-Darcian effects on double-diffusive convection inside porous square cavity. Recently Bennacer et al.[24] assessed the double-diffusive free convection in a tunnel stuffed with anisotropic porous matrix. Taking into account the sinusoidal barrier conditions, Mansour et al.[25] abstracted the double diffusion through an inclined triangular penetrable zone. Rashad et al.[26] also discussed the sinusoidal perimeter conditions at the lower wall for the impact of radiation and chemical reaction through a square enclosure. An analysis was carried out numerically by Ahmed et al.[27] to study unsteady heat and mass transfer by free convection flow of a viscous, incompressible, electrically conducting Newtonian fluid along a vertical permeable plate under the action of transverse magnetic field taking into account thermal radiation as well as homogeneous chemical reaction of first order. They investigated that the local skin friction and the Sherwood number were considerably increased with an increase in the chemical reaction parameter.

Umavathi and Monica[28] investigated the double diffusion using nanofluid in a permeable matrix with cross diffusion and conductivity. Umavathi[29] probed the combined reaction of heat conductivity and viscosity on double-diffusion. Also Umavathi and research group[30–32] worked on the double diffusion in a fibrous layer saturated with an Oldroyed nanofluid. Later, Prathap kumar et al.[33] worked on double diffusion convection with nanofluid in vertical duct. The numerical solution of 2-D unsteady free convective heat and mass transfer flow over a moving semi-infinite vertical porous plate with thermal diffusion in presence of magnetic field, dissipative heat and Soret effects taking into account the induced magnetic field was designed by Zueco et al.[34] It was determined that an increase in the Soret or Eckert number was found to strongly enhance the fluid velocity and temperature values, and this effect was reversed for the induced magnetic field. It was also found that the flow velocity decreases with the increase in Hartmann and magnetic Prandtl number, and an opposite behavior was observed for the fluid temperature.

In all the analysis reported above, the heat exchange at the exterior was not considered. In many application such as engineering and industrial field convective heat exchange becomes needful. Thus, many authors Aziz,[35]

ARTICLE

ARTICLE

Aziz et al.,[36] Makinde et al.,[37] Ahmad and Khan[38] reported enforcing the convective boundary conditions. Also, the researchers Wibulswal,[39] Lyczkowski et al.[40] and Javeri[41] abstracted the flow properties through a rectangular carrier for the isothermal heating, Hicken[42] and Sparrow and Sparrow and Siegel[43] followed second kind barrier heat.

Javeri[44,45] scrutinized momentum and energy maintaining the Fourier-type bounded conditions past a flat plate and in a rectangular avenue. Uniform plate temperature and Robin edge conditions in a vertical carrier was inspected by Barletta[46] and Zanchini[47] respectively. Mahanti and Gaur[48] reviewed the significance of viscosity and conductivity of heat for the flow in vertical conduit for isothermal bounded conditions. Following Barletta[46] and Zanchini[47], Umavathi[49–59] researched the convection in a passage (single and double) approving Fourier-type barrier conditions.

Technical literature describing the deployment of nanofluids in duct flows to estimate the convection for two diffusing components is limited. This has prompted the present investigation in which the *deployment of aqueous nanofluids in a vertical duct with thermo-solutal convection and cross diffusion effects is considered for the first time* using Fourier-type edge heating adopting two phase model. All these aspects constitute the novelty of the present article. In this work the double-diffusion of nanofluid using Fourier-type edge heating is inspected. The outcome of this work is relevant in electronics, transport networks, biomedical etc.

2. MATHEMATICAL FORMULATION

The physical structure is plotted in the Figure 1. The thermosolutal natural convection in a vertical long two dimensional duct filled with nanofluid is solved incorporating the convective edge conditions. The two barriers are detached at a width L. The X-axis is lateral to the walls and is in opposite direction to gravity. Also the Y-axis is normal to walls. The duct occupies the area $-L/2 \le Y \le L/2$. The surfaces are maintained at constant temperature and concentration T_1, C_1 and T_2, C_2. The viscosity, heat conductivity and heat expansion are guessed to be constant. In addition, viscous dissipation, Brownian motion, thermopheresis, Soret and Schmidt effects is considered. The flow is flourished with the buoyancy forces. No slip conditions on the velocity is imposed. The Newton's conservation laws of mass, momentum, energy and concentration of species and nonoparticles volume fraction equations are written as follows (Buongionrno,[9] Javeri[33] and Nithiarasu et al.[17]).

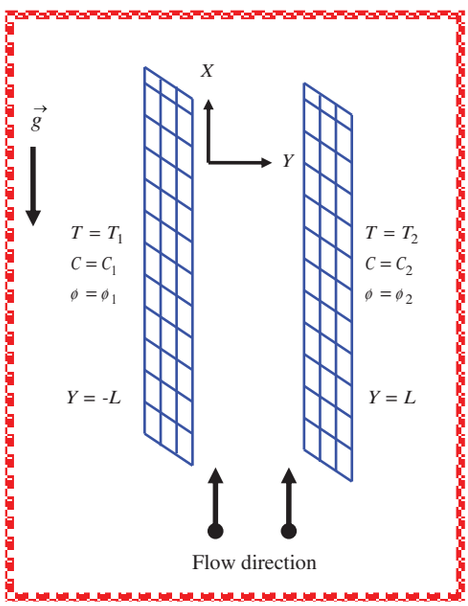

Fig. 1. Physical configuration.

$$\beta_T g(T - T_0) + \beta_C g(\phi^* - \phi^*_0) - \frac{1}{\rho_0}\frac{\partial P}{\partial X} + \nu\frac{d^2U}{dY^2} = 0 \quad (1)$$

$$\alpha\frac{d^2T}{dY^2} + \tau\left[D_B\left(\frac{\partial C}{\partial Y}\frac{\partial T}{\partial Y}\right) + \frac{D_T}{T_\infty}\left(\frac{\partial T}{\partial Y}\right)^2\right] + \frac{\upsilon}{C_P}\left(\frac{dU}{dY}\right)^2 = 0 \quad (2)$$

$$D_B\frac{d^2C^*}{dY^2} + \frac{D_T}{T_\infty}\frac{d^2T}{dY^2} = 0 \quad (3)$$

$$D_m\frac{d^2\phi^*}{dY^2} + \frac{kD_m}{T}\frac{d^2T}{dY^2} = 0 \quad (4)$$

The associated conditions are

$$u\left(-\frac{L}{2}\right) = u\left(\frac{L}{2}\right) = 0 \quad (5)$$

$$-k\left.\frac{\partial T}{\partial Y}\right|_{-L/2} = h_1\left[T_1 - T\left(X, -\frac{L}{2}\right)\right] \quad (6)$$

$$-k\left.\frac{\partial T}{\partial Y}\right|_{L/2} = h_2\left[T\left(X, \frac{L}{2}\right) - T_2\right] \quad (7)$$

$$C^* = C_1 \quad \text{at} \quad Y = -\frac{L}{2} \quad \text{and} \quad C^* = C_2 \quad \text{at} \quad Y = \frac{L}{2} \quad (8)$$

$$\phi^* = \phi_1 \quad \text{at} \quad Y = -\frac{L}{2} \quad \text{and} \quad \phi^* = \phi_2 \quad \text{at} \quad Y = \frac{L}{2} \quad (9)$$

The above equations are rephrases in a non-dimensional form by introducing the relations

$$u = \frac{U}{U_0}, \quad \theta = \frac{T - T_0}{\Delta T}, \quad y = \frac{Y}{D}, \quad GR_T = \frac{g\beta_T\Delta TD^3}{\upsilon^2},$$

$$GR_\phi = \frac{g\beta_\phi\Delta\phi D^3}{\upsilon^2}, \quad Br = \frac{\mu U_0^2}{k\Delta T}, \quad Pr = \frac{\upsilon}{\alpha},$$

$$Re = \frac{U_0 D}{\upsilon}, \quad \Lambda_1 = \frac{GR_T}{Re}, \quad \Lambda_2 = \frac{GR_\phi}{Re},$$

$$Nb=\frac{(\rho C)_P D_B (C_2-C_1)}{(\rho C)_f \upsilon},\quad Nt=\frac{(\rho C)_P D_T (T_2-T_1)}{(\rho C)_f \upsilon T_\infty},$$
$$\phi=\frac{\phi^*-\phi^*_0}{\Delta\phi},\quad C=\frac{C^*-C^*_0}{\Delta C},\quad Sc=\frac{\upsilon}{D_m},\qquad (10)$$
$$Sr=\frac{k\Delta T D_m}{T\upsilon\Delta\phi},\quad Bi_1=\frac{h_1 D_1}{k_1},\quad Bi_2=\frac{h_2 D_2}{k_2},$$
$$R_T=\frac{T_2-T_1}{\Delta T},\quad S=\frac{Bi_1 Bi_2}{Bi_1 Bi_2+2Bi_1+2Bi_2},$$
$$Ec=\frac{\mu^2}{C_p\Delta T},\quad Le=\frac{\upsilon}{D_B},\quad U_0=\frac{-AD^2}{48\mu}$$

Here $D=2L$ is the diameter. The reference velocity, temperature and concentration are written as,

$$U_0=-\frac{AD^2}{48\mu},\quad T_0=\frac{T_1+T_2}{2}+S\left(\frac{1}{Bi_1}-\frac{1}{Bi_2}\right)[T_2-T_1],\qquad (11)$$
$$C_0=\frac{C_1+C_2}{2}$$

Here $\Delta T=T_2-T_1$, if $T_1<T_2$ and $\Delta C=C_2-C_1$ if $C_1<C_2$. Therefore, the reference temperature field difference $\Delta T=\nu^2/(C_pD^2)$, if $T_1=T_2$. Hence, if $T_1<T_2$ then $R_T=1$ and if $T_1=T_2$ then $R_T=0$

The Eqs. (1)–(9) in non-dimensional form reduce to

$$\frac{d^2u}{dy^2}=-48-\Lambda_1\theta-\Lambda_2\phi \qquad (12)$$

$$\frac{d^2\theta}{dy^2}+Nb\ Pr\frac{dC^*}{dy}\frac{d\theta}{dy}+Nt\ Pr\left(\frac{d\theta}{dy}\right)^2+Ec\ Pr\left(\frac{du}{dy}\right)^2=0 \qquad (13)$$

$$\frac{d^2C}{dy^2}+\frac{Nt}{Nb}\frac{d^2\theta}{dy^2}=0 \qquad (14)$$

$$\frac{d^2\phi}{dy^2}+Sc\ Sr\frac{d^2\theta}{dy^2}=0 \qquad (15)$$

$$u(-1/4)=u(1/4)=0 \qquad (16)$$

$$\left.\frac{d\theta}{dy}\right|_{y=-1/4}=Bi_1\left[\theta+\frac{R_TS}{2}\left(1+\frac{4}{Bi_1}\right)\right] \qquad (17)$$

$$\left.\frac{d\theta}{dy}\right|_{y=1/4}=Bi_2\left[-\theta+\frac{R_TS}{2}\left(1+\frac{4}{Bi_2}\right)\right] \qquad (18)$$

$$C\left(-\frac{1}{4}\right)=-\frac{1}{2},\quad C\left(\frac{1}{4}\right)=\frac{1}{2} \qquad (19)$$

$$\phi\left(-\frac{1}{4}\right)=-\frac{1}{2},\quad \phi\left(\frac{1}{4}\right)=\frac{1}{2} \qquad (20)$$

3. SOLUTIONS

The analytical solutions are accomplished affiliating perturbation technique considering Prandtl number as the perturbation parameter. The solutions of Eqs. (12)–(15) can be written as.

$$u(y)=u_0(y)+Pr\ u_1(y)+Pr^2u_2(y)+\ldots \qquad (21)$$

$$\theta(y)=\theta_0(y)+Pr\ \theta_1(y)+Pr^2\theta_2(y)+\ldots \qquad (22)$$

$$C(y)=C_0{}^*(y)+Pr\ C_1{}^*(y)+Pr^2C_2{}^*(y)+\ldots \qquad (23)$$

$$\phi(y)=\phi_0(y)+Pr\ (y)=\phi_1(y)+Pr^2\phi_2(y)+\ldots \qquad (24)$$

Substituting Eqs. (21)–(24) into Eqs. (12)–(20), and then comparing the like powers of Prandtl number generates the sequence of boundary value problem for u, θ, C and ϕ which are detailed below.

The Eqs. (12)–(20) when $Pr=0$ are

$$\frac{d^2u_0}{dy^2}=0 \qquad (25)$$

$$\frac{d^2\theta_0}{dy^2}=0 \qquad (26)$$

$$\frac{d^2C_0}{dy^2}=0 \qquad (27)$$

$$\frac{d^2\phi_0}{dy^2}=0 \qquad (28)$$

along with the conditions

$$u_0\left(-\frac{1}{4}\right)=u_0\left(\frac{1}{4}\right)=0 \qquad (29)$$

$$\left.\frac{d\theta_0}{dy}\right|_{y=-1/4}=Bi_1\left[\theta_0+\frac{R_TS}{2}\left(1+\frac{4}{Bi_1}\right)\right] \qquad (30)$$

$$\left.\frac{d\theta_0}{dy}\right|_{y=1/4}=Bi_2\left[-\theta_0+\frac{R_TS}{2}\left(1+\frac{4}{Bi_2}\right)\right] \qquad (31)$$

$$C_0\left(-\frac{1}{4}\right)=-\frac{1}{2},\quad C_0\left(\frac{1}{4}\right)=\frac{1}{2} \qquad (32)$$

$$\phi_0\left(-\frac{1}{4}\right)=-\frac{1}{2},\quad \phi_0\left(\frac{1}{4}\right)=\frac{1}{2} \qquad (33)$$

The solutions u_0, θ_0, C_0 and ϕ_0 are obtained by integrating the Eqs. (25)–(28) using the Eqs. (29)–(33).

The equations for $n>0$ are evolved as

$$\frac{d^2u_n}{dy^2}=\sum_{n=0}^{\infty}\Lambda_1\theta_n+\sum_{n=0}^{\infty}\Lambda_2\phi_n \qquad (34)$$

$$\frac{d^2\theta_n}{dy^2}=\sum_{j=0}^{n-1}Nb\frac{dC^*{}_j}{dy}\frac{d\theta_{n-j-1}}{dy}+\sum_{j=0}^{n-1}Nt\frac{d\theta_j}{dy}\frac{d\theta_{n-j-1}}{dy}+\sum_{j=0}^{n-1}Ec\frac{du_j}{dy}\frac{du_{n-j-1}}{dy} \qquad (35)$$

$$\frac{d^2C_n}{dy^2}=\frac{Nt}{Nb}\frac{d^2\theta_n}{dy^2} \qquad (36)$$

$$\frac{d^2\phi_n}{dy^2}=\frac{Nt}{Nb}\frac{d^2\theta_n}{dy^2} \qquad (37)$$

with the boundary conditions

$$u_n\left(-\frac{1}{4}\right) = u_n\left(\frac{1}{4}\right) = 0 \tag{38}$$

$$\left.\frac{d\theta_n}{dy}\right|_{y=-1/4} = Bi_1\left[\theta_n\right] \tag{39}$$

$$\left.\frac{d\theta_n}{dy}\right|_{y=1/4} = Bi_2\left[-\theta_n\right] \tag{40}$$

$$C_n\left(-\frac{1}{4}\right) = C_n\left(\frac{1}{4}\right) = 0 \tag{41}$$

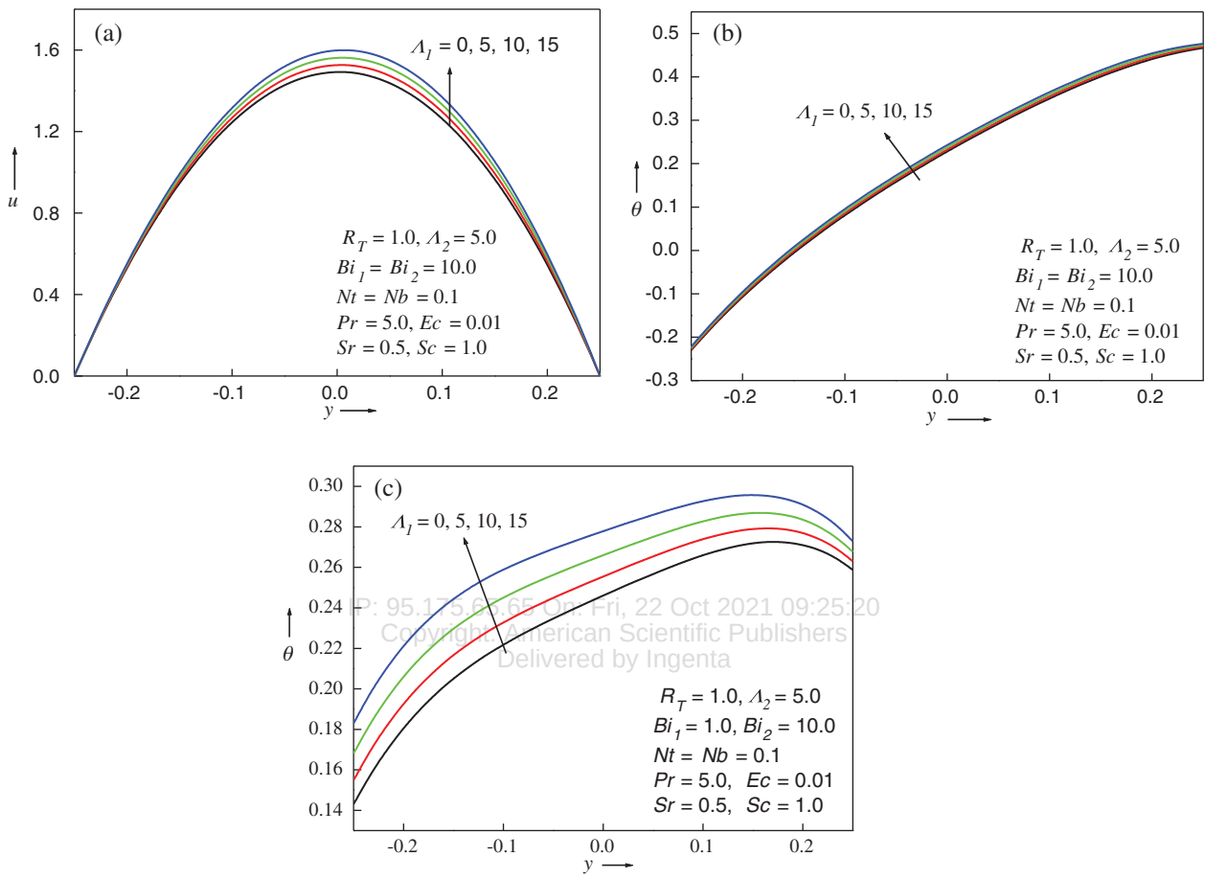

Fig. 2. (a) Impact of Λ_1 on the velocity with equal Biot numbers. (b) Impact of Λ_1 on the temperature with equal Biot numbers. (c) Impact of Λ_1 on the temperature with unequal Biot numbers.

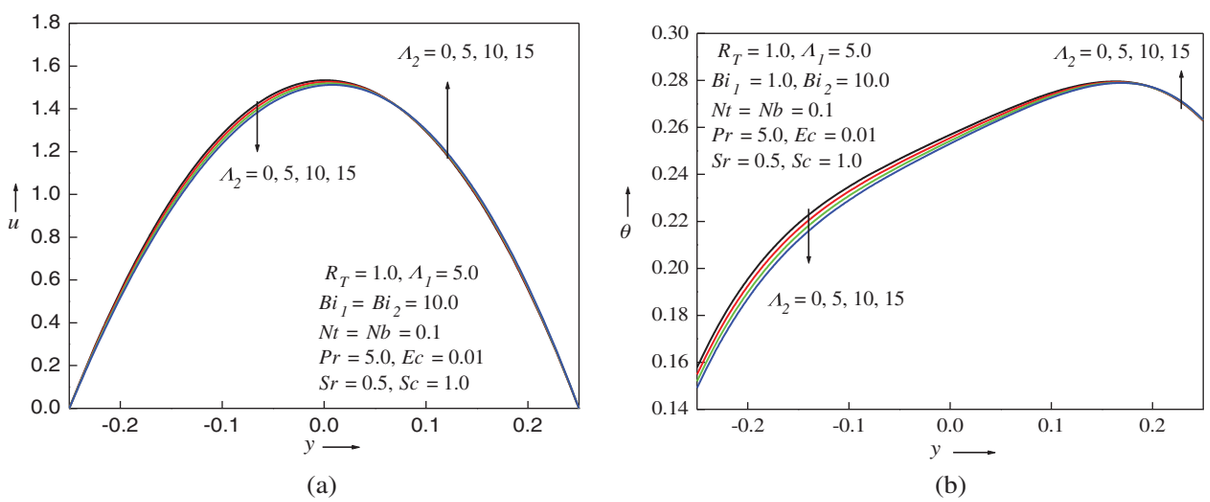

Fig. 3. (a) Impact of Λ_2 on the velocity with unequal Biot numbers. (b) Impact of Λ_2 on the temperature with unequal Biot numbers.

$$\phi_n\left(-\frac{1}{4}\right)=\phi_n\left(\frac{1}{4}\right)=0 \tag{42}$$

The solutions of Eqs. (34)–(37) along with Eqs. (38)–(42) are acquired by the iteration procedure. The solutions of u_0, θ_0, C_0 and ϕ_0 are substituted to produce the solutions for u_1, θ_1, C_1 and ϕ_1 $(n=1)$. Substituting u_1, θ_1, C_1 and ϕ_1 the solutions of u_2, θ_2, C_2 and $\phi_2(n=2)$ are acquired and the process is continued till the desired value of n.

The non-dimensional Nusselt number, Skin friction, Sherwood number, average velocity and bulk temperature are set out as follows.

$$Nu_1=\frac{1}{R_T\left[\theta\left(\frac{1}{4}\right)-\theta\left(-\frac{1}{4}\right)\right]+(1-R_T)}\left(\frac{d\theta}{dy}\right)_{y=-1/4} \tag{43}$$

$$Nu_2=Nu_1=\frac{1}{R_T\left[\theta\left(\frac{1}{4}\right)-\theta\left(-\frac{1}{4}\right)\right]+(1-R_T)}\left(\frac{d\theta}{dy}\right)_{y=1/4} \tag{44}$$

$$\tau_1=\left(\frac{du}{dy}\right)_{y=-1/4},\quad \tau_2=\left(\frac{du}{dy}\right)_{y=1/4} \tag{45}$$

$$Sh_1=\left(\frac{d\phi}{dy}\right)_{y=-1/4},\quad Sh_2=\left(\frac{d\phi}{dy}\right)_{y=1/4} \tag{46}$$

$$\overline{u}=2\int_{-1/4}^{1/4}u\,dy \tag{47}$$

$$\theta_b=\frac{2}{\overline{u}}\int_{-1/4}^{1/4}u\,\theta\,dy \tag{48}$$

4. RESULTS AND DISCUSSION

The equations resolved are nonlinear and there are no possibilities to find the closed form solutions. Hence approximate solutions are attained using Prandtl number as the perturbation parameter. To relax this condition on Prandtl number, the equations are computed applying Runge-Kutta-Shooting method. The values obtained by Runge-Kutta-Shooting are justified with the perturbation solutions.

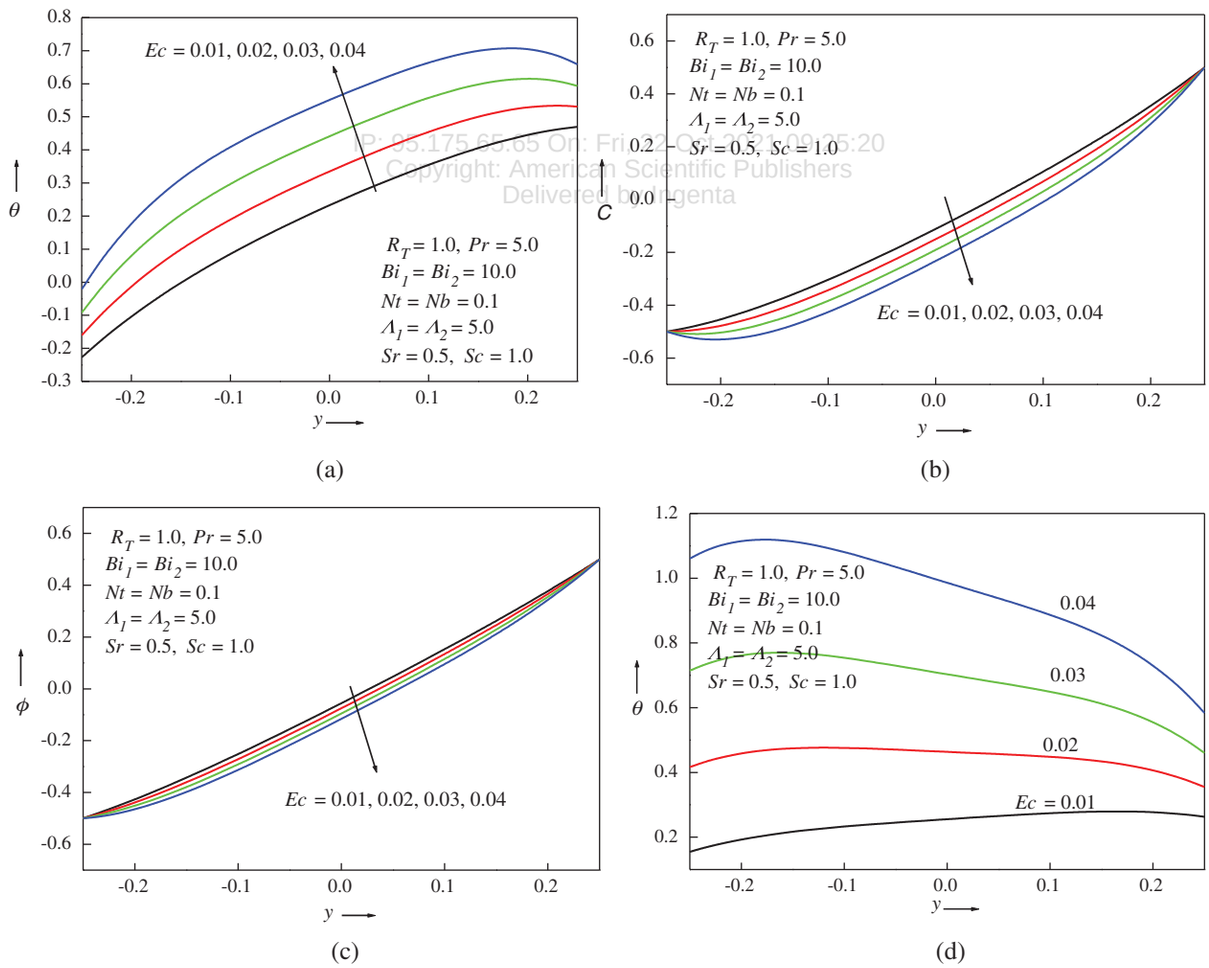

Fig. 4. (a) Impact of Ec on the temperature with equal Biot numbers. (b) Impact of Ec on the Concentration with equal Biot numbers. (c) Impact of Ec on the nanoparticle volume fraction for equal Biot numbers. (d) Impact of Ec on the temperature with unequal Biot numbers.

ARTICLE

The pictorial results under the investigation are depicted in Figures 2–6. Figures 2(a)–(c) example the reaction of Λ_1 on the flow. As Λ_1 gets boosted, the momentum and temperature values (Figs. 2(a and b)) are also hiked. The physical insight is that the Λ_1 operates as a dynamic force to gain the momentum. This also accelerates the viscous dissipation and hence enlarges the thermal fields. Figure 2(c) demonstrate that the magnitude of upsurge is significant for dissimlar Biot numbers in correlation with uniform Biot numbers. The consequence of Λ_1 on C, ϕ do not show sizable changes for all values of Biot numbers and also the effect of Λ_1 on the velocity for different Biot numbers is congruent to that of similar Biot number and are not placed in graphs. As the mass Grashof number Λ_2 increases, the velocity declines at the cold wall and increases slightly at the hot plate (Fig. 3(a)) for $Bi_1 = Bi_2 = 10$. The effect of Λ_2 on θ for $Bi_1 = Bi_2 = 10$ do not alter the field significantly and hence not shown but it influences for $Bi_1 = 1, Bi_2 = 10$ as seen in Figure 3(b). This figure ascertain that Λ_2 decreases the heat and its impact is more at the cold wall. The influence of Λ_2 on the velocity for $Bi_1 = 1, Bi_2 = 10$ is similar to $Bi_1 = Bi_2 = 10$ and the impact of Λ_2 on C and ϕ for similar and different Biot numbers do not display any major changes and hence not displayed.

Figures 4(a)–(d) show the effect of Ec on the flow. Eckert number specifies the relative productiveness of heat dissipation transport by diffusion on the velocity field, temperature field, nanoparticle volume fraction filed and concentration field. As Ec is surged velocity is also boosted for all values of Biot numbers which is same as Figure 2(a) and hence not shown pictorially. Figure 4(a) ($Bi_1 = Bi_2 = 10$) and 4(d) ($Bi_1 = 1, Bi_2 = 10$) are the heat profiles and it shows that the heat is hiked as Ec increases. However the nature of upsurge is different for different Bi. The utmost hike of θ is attained at the cold wall for $Bi_1 = 1, Bi_2 = 10$. As Ec increases the C (Fig. 4(b)) and ϕ (Fig. 4(c)) are decreased for equal values of Bi. Similar

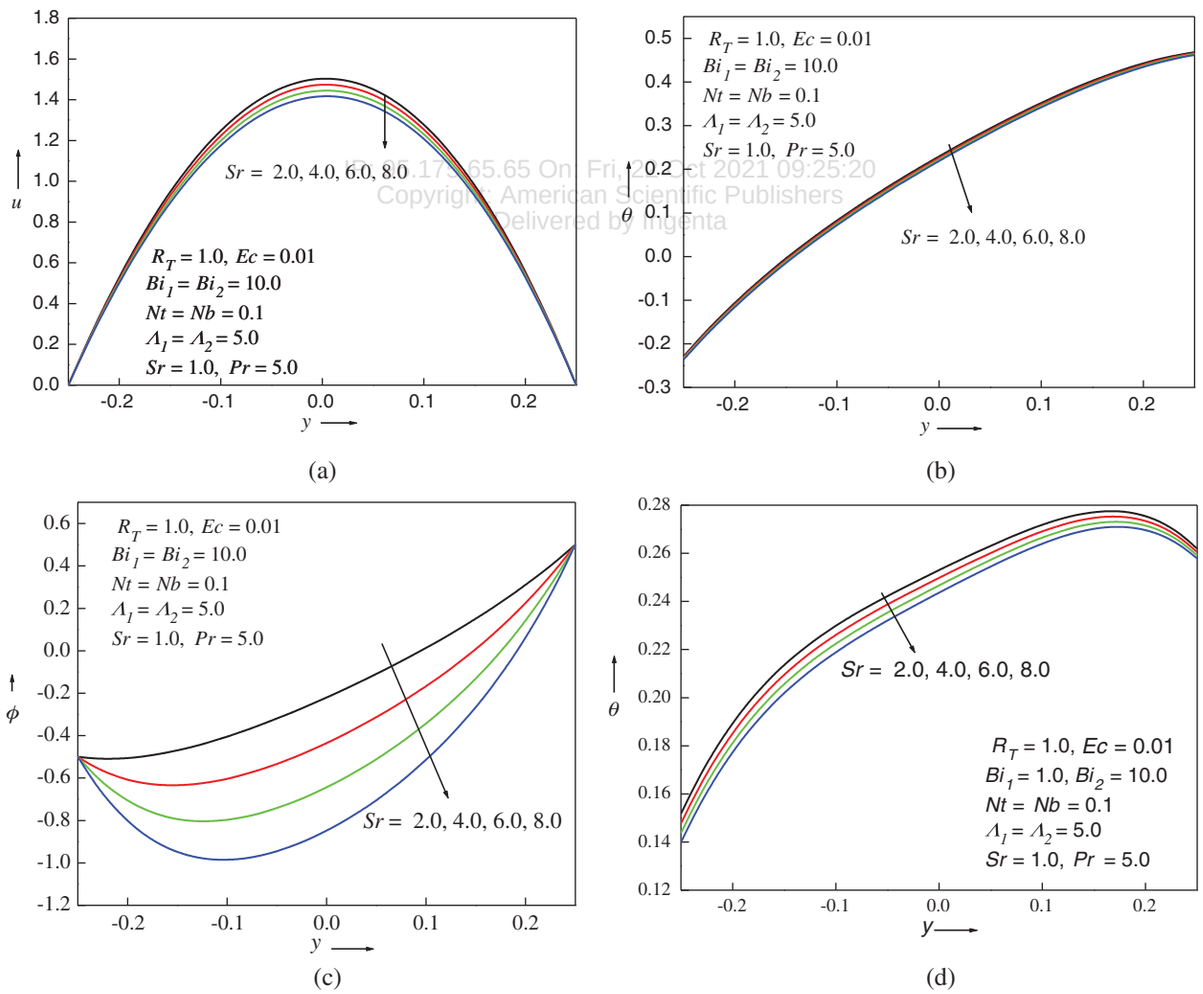

Fig. 5. (a) Impact of Sr on the velocity with equal Biot numbers. (b) Impact of Sr on the temperature with equal Biot numbers. (c) Impact of Sr on the Concentration with equal Biot numbers. (d) Temperature profiels for Sr with unequal Biot numbers.

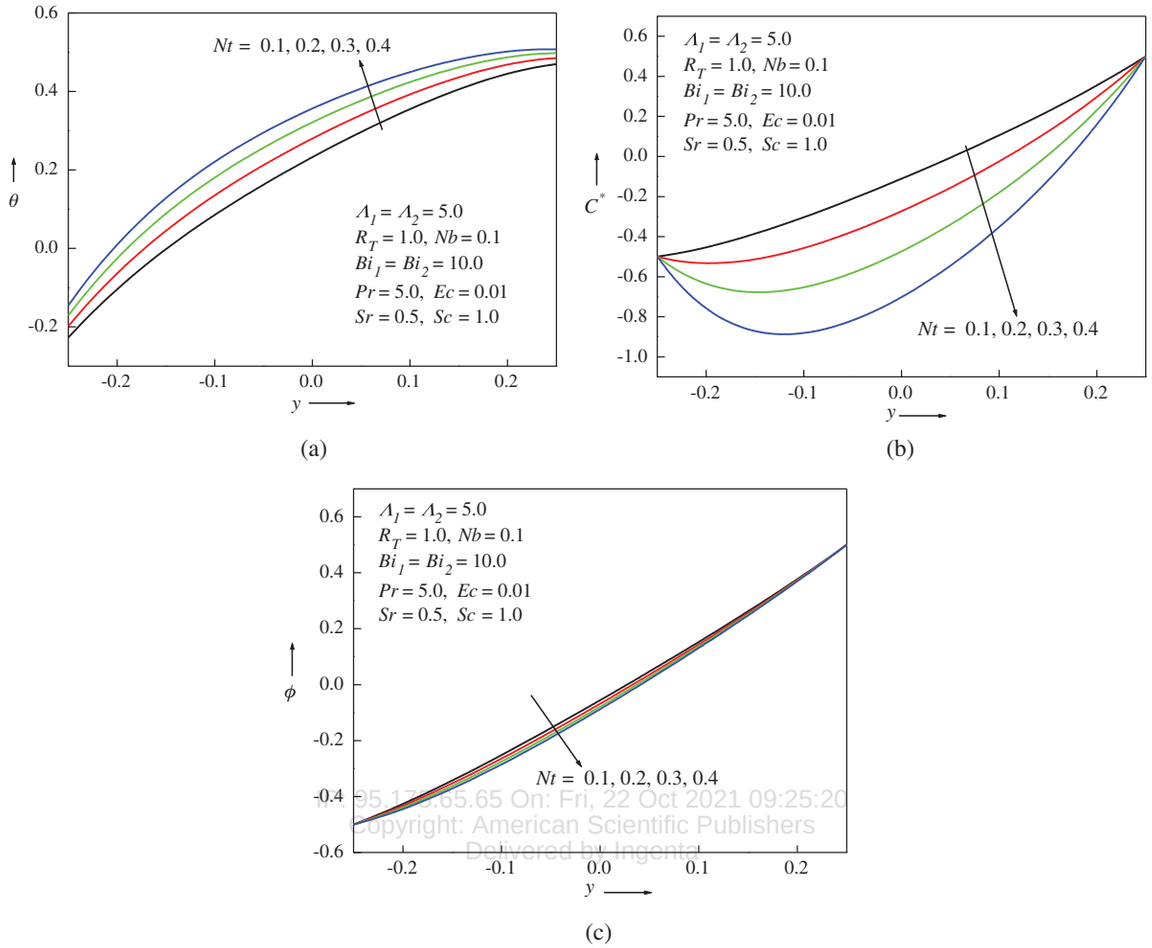

Fig. 6. (a) Impact of Nt on the temperature with equal Biot numbers. (b) Impact of Nt on the nanoparticle volume fraction with equal Biot numbers. (c) Impact of Nt on the Concentration with equal Biot numbers.

profiles are attained for unequal values of Bi and hence not shown. The effect of Pr is same as Ec and hence not figured.

Figures 5(a)–(d) show the effects of Soret parameter. As the Sr increases u, θ, ϕ are suppressed for $Bi_1 = Bi_2 = 10$ (Figs. 5(a–c)). The reaction of Sr on C shows the similar profiles as that on θ and not depicted for $Bi_1 = Bi_2 = 10$. The role of Sr also reduces θ for $Bi_1 = 1, Bi_2 = 10$ but the magnitude of reduction is dense in comparison with $Bi_1 = Bi_2 = 10$. The effect of Sr on u, C, ϕ for $Bi_1 = 1, Bi_2 = 10$ is similar to $Bi_1 = Bi_2 = 10$. Effect of Sc is similar to Sr.

The momentum is not responsive with the presence of Nt. The effect of Nt on θ is to amplify the temperature whereas it suppresses C and ϕ as seen in Figures 6(a)–(c) for $Bi_1 = Bi_2 = 10$. The results for $Bi_1 = 1, Bi_2 = 10$ are same as for $Bi_1 = 1, Bi_2 = 10$. The reflex of Nb is similar to Nt except on the concentration. Figure 7 expo that as Nb expands, C is also enlarged for related Biot numbers and similar nature is attained for unrelated Biot numbers. The significance of Nb on u, θ, ϕ is similar to Nt.

Table I shows the comparison of numerical and analytical solutions. The analytical solutions are computed considering seven terms of the perturbation series. The table infers that in the absence of Prandtl number (perturbation

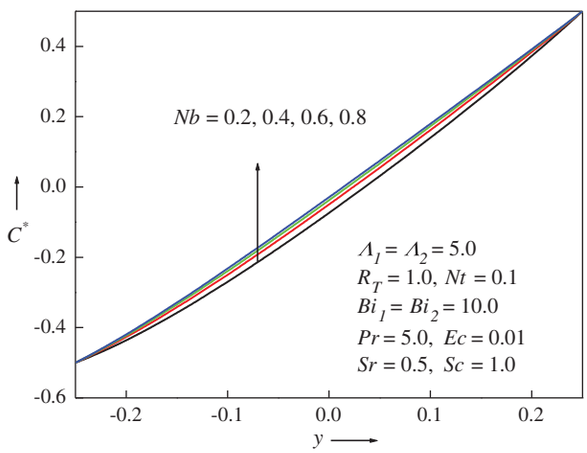

Fig. 7. Impact of Nb on the nanoparticle volume fraction with equal Biot numbers.

ARTICLE

Table I. Values of velocity with series expansion up to seven terms.

	$Bi_1 = Bi_2 = 10$ $u = u_0 + Pr\,u_1 + Pr^2u_2 + Pr^3u_3 + Pr^4u_4 + Pr^5u_5 + Pr^6u_6 + Pr^7u_7$					
	$Pr = 0$		$Pr = 0.01$		$Pr = 0.5$	
y	Analytical	Numerical	Analytical	Numerical	Analytical	Numerical
−0.25	0.00000000	0.00000000	0.00000000	0.00000000	0.00000000	0.00000000
−0.15	0.94285714	0.94285714	0.94382755	0.94364361	0.99186496	0.98571341
−0.05	1.43142857	1.43142857	1.43290497	1.43261964	1.50589094	1.49627108
0.05	1.44857143	1.44857143	1.45005011	1.44976469	1.52305017	1.51347262
0.15	0.97714286	0.97714286	0.97811817	0.97793389	1.02620791	1.02012797
0.25	0.00000000	0.00000000	0.00000000	0.00000000	0.00000000	0.00000000
y	$Bi_1 = 1.0, Bi_2 = 10$					
	$Pr = 0$		$Pr = 0.01$		$Pr = 0.5$	
	Analytical	Numerical	Analytical	Numerical	Analytical	Numerical
−0.25	0.00000000	0.00000000	0.00000000	0.00000000	0.00000000	0.00000000
−0.15	0.94687500	0.94687500	0.94784541	0.94899852	0.99588282	1.08153328
−0.05	1.43343750	1.43343750	1.43491390	1.43646476	1.50789987	1.62524576
0.05	1.44656250	1.44656250	1.44804117	1.44942301	1.52104124	1.62765845
0.15	0.97312500	0.97312500	0.97410031	0.97491515	1.02219005	1.08636038
0.25	0.00000000	0.00000000	0.00000000	0.00000000	0.00000000	0.00000000

Table II. Value of Nusselt numbers, mean velocity and bulk temperature.

	$Bi_1 = Bi_2 = 10$				$Bi_1 = 1.0,\ Bi_2 = 10$			
	Nu_1	Nu_2	$\overline{u}$	θ_b	Nu_1	Nu_2	$\overline{u}$	θ_b
Λ_1								
0	6.19321	−2.30891	0.99075	0.48502	−3.69838	7.85776	0.99096	1.06361
5	6.12896	−2.32614	1.04116	0.48605	−3.72200	7.93296	1.10167	1.06246
10	6.06623	−2.34395	1.09162	0.48711	−3.74591	8.00928	1.21204	1.06123
15	6.00499	−2.36235	1.14217	0.48822	−3.77008	8.08676	1.32208	1.05996
Λ_2								
0	6.21932	−2.30216	1.05039	0.48459	−3.64736	7.69626	1.11129	1.06884
5	6.12896	−2.32614	1.04116	0.48605	−3.72200	7.93296	1.10167	1.06246
10	6.04156	−2.35122	1.03193	0.48773	−3.79946	8.18127	1.09209	1.05652
15	5.95705	−2.37737	1.02269	0.48965	−3.87981	8.44173	1.08251	1.05101
Ec								
0.2	3.71679	0.203658	1.01704	0.20304	−49.3418	55.2152	1.04111	0.42998
0.4	5.32945	−1.48764	1.03312	0.39171	−4.72678	8.97434	1.08149	0.85154
0.6	6.92398	−3.15994	1.0491979	0.58038	−3.20245	7.39447	1.12186	1.27346
0.8	8.50069	−4.81355	1.06528	0.76905	−2.67093	6.84358	1.16223	1.69570
Pr								
0.0	2.00000	2.00000	1.00000	0.00212	2.00000	2.00000	1.00000	0.00071
0.01	2.08374	1.91227	1.00082	0.01180	2.20054	1.79207	1.00203	0.02192
0.5	6.12896	−2.32614	1.04116	0.48605	−3.72200	7.93296	1.10167	1.06246
1.0	10.1432	−6.53212	1.08232	0.96998	−2.39694	6.55904	1.20335	2.12639
Nb								
0.5	6.32614	−2.52333	1.04339	0.51462	−3.65096	7.85499	1.10393	1.08727
1.0	6.57262	−2.76981	1.04618	0.55033	−3.35846	7.76446	1.10676	1.11828
1.5	6.81910	−3.01629	1.04897	0.58604	−3.49219	7.68078	1.10958	1.14929
2.0	7.06558	−3.26276	1.05176	0.62175	−3.42151	7.60320	1.11240	1.18030
Nt								
0.5	6.26981	−2.46699	1.04275	0.50645	−3.69929	7.90803	1.10238	1.07021
1.0	6.44586	−2.64305	1.04475	0.53196	−3.67156	7.87760	1.10326	1.07990
1.5	6.62192	−2.81910	1.04674	0.55747	−3.64454	7.84795	1.10414	1.08959
2.0	6.79798	−2.99516	1.04873	0.58298	−3.61820	7.81905	1.10503	1.09928

Table II. Continued.

	$Bi_1 = Bi_2 = 10$				$Bi_1 = 1.0,\ Bi_2 = 10$			
	Nu_1	Nu_2	$\overline{u}$	θ_b	Nu_1	Nu_2	$\overline{u}$	θ_b
Sc								
0.5	6.12896	−2.32614	1.04578	0.48604	−3.72200	7.93296	1.10619	1.06246
1.0	6.12896	−2.32614	1.04116	0.48605	−3.72200	7.93296	1.10167	1.06246
1.5	6.12896	−2.32614	1.03653	0.48605	−3.72200	7.93296	1.09715	1.06246
2.0	6.12896	−2.32614	1.03190	0.48606	−3.72200	7.93296	1.09264	1.06245
Sr								
0.5	6.12896	−2.32614	1.04116	0.48605	−3.72200	7.93296	1.10167	1.06246
1.0	6.12896	−2.32614	1.03190	0.48607	−3.72200	7.93296	1.09264	1.06245
1.5	6.12896	−2.32614	1.02265	0.48607	−3.72200	7.93296	1.08359	1.06244
0	6.12896	−2.32614	1.01339	0.48608	−3.72200	7.93296	1.07456	1.06243

Table III. Values of skin friction.

	$Bi_1 = Bi_2 = 10$		$Bi_1 = 1.0,\ Bi_2 = 10$	
	τ_1	τ_2	τ_1	τ_2
Λ_1				
0	11.69486	−10.21273	11.69698	−10.21485
5	12.12031	−11.01463	13.10595	−11.35380
10	12.54417	−11.82040	14.50879	−12.49157
15	12.96676	−12.63035	15.90565	−13.62828
Λ_2				
0	12.42666	−10.79955	13.41911	−11.14115
5	12.12031	−11.01463	13.10595	−11.35380
10	11.81431	−11.22934	12.79351	−11.56628
15	11.50853	−11.44356	12.48165	−11.77848
Ec				
0.2	11.84034	−10.73378	12.28424	−10.79179
0.4	12.02699	−10.92102	12.83205	−11.16644
0.6	12.21363	−11.10825	13.37986	−11.54115
0.8	12.40028	−11.29548	13.92766	−11.91586
Pr				
0.0	11.64285	−10.53514	11.72656	−10.41015
0.01	11.65241	−10.54529	11.75415	−10.42902
0.5	12.12031	−11.01463	13.10595	−11.35380
1.0	12.59778	−11.49356	14.48535	−12.29736
Nb				
0.5	12.14561	−11.04351	13.13607	−11.37749
1.0	12.17724	−11.07557	13.17371	−11.40403
1.5	12.20885	−11.10735	13.21134	−11.43034
2.0	12.24047	−11.13904	13.24898	−11.45658
Nt				
0.5	12.13838	−11.01485	13.11536	−11.34668
1.0	12.16097	−11.01512	13.12713	−11.33778
1.5	12.18356	−11.01538	13.13889	−11.32887
2.0	12.20615	−11.01565	13.15065	−11.31996
Sc				
0.5	12.16868	−11.06331	13.15328	−11.40136
1.0	12.12031	−11.01463	13.10596	−11.35380
1.5	12.07194	−10.96596	13.05863	−11.30624
2.0	12.02358	−10.91729	13.01131	−11.25868
Sr				
0.5	12.12031	−11.01463	13.10596	−11.35380
1.0	12.02358	−10.91729	13.01131	−11.25868
1.5	11.92685	−10.81994	12.91665	−11.16362
2.0	11.83012	−10.72259	12.82201	−11.06844

ARTICLE

parameter) the perturbation and Shooting values are equal upto eight decimal places. For $Pr = 0.01$, the values agree upto two decimal places and for $Pr = 0.5$ they agree upto one decimal place when $Bi_1 = Bi_2 = 10$. The difference is large for $Bi_1 = 1, Bi_2 = 10$ in comparison with $Bi_1 = Bi_2 = 10$.

The Nusselt values on the left wall decreases with increase in Λ_1, Λ_2 whereas it increases with boosting Ec, Pr, Nb, Nt for any values of Biot numbers as tabulated in Table II. The impact of Λ_1, Λ_2, Ec, Pr, Nb, Nt diminishes Nu at the hot plate for same Biot numbers. For different Biot numbers Λ_1, Λ_2 promotes the heat transfer and Ec, Pr, Nb, Nt decreases the Nusselt values at the right plate. The average velocity is hiked with Λ_1, Ec, Pr, Nb, Nt and decreases with Λ_2 for all values of Bi. The bulk temperature increases with the parameters Λ_1, Λ_2, Ec, Pr, Nb, Nt for equal Biot numbers. It decreases with Λ_1, Λ_2 and increases with Ec, Pr, Nb, Nt for unequal Biot numbers. The influence of Sc and Sr do not alter the Nusselt, average velocity and bulk temperature and are not tabulated.

In Table III it is seen that the skin friction is up surged with Λ_1, Ec, Pr, Nb, Nt whereas it is down streamed with Λ_2, Sc, Sr for all values of Bi. The skin friction at the right plate decreases with Λ_1, Λ_2, Ec, Pr, Nb, Nt and increases with Sc, Sr for equal Biot numbers. For unequal Biot number it decreases with Λ_1, Λ_2, Ec, Pr, Nb and increases with Nt, Sc, Sr. Shear wood number at the left plate decreases with Λ_1, Ec, Pr, Nt and increases

Table IV. Values of Sherwood numbers.

	$Bi_1 = Bi_2 = 10$		$Bi_1 = 1.0, Bi_2 = 10$	
	Sh_1	Sh_2	Sh_1	Sh_2
Λ_1				
0	−0.99260020	5.02297649	−0.90202684	4.97006480
5	−1.29309968	5.38461599	−1.80994558	5.82343923
10	−1.70249430	5.86337760	−4.52952651	8.31350155
15	−2.30585136	6.54830775	−0.36970454	10.3087813
Λ_2				
0	−1.40576513	5.40920047	−1.97162973	5.88692991
5	−1.29309968	5.38461599	−1.80994558	5.82343923
10	−1.18613584	5.36383692	−1.65963985	5.76846119
15	−1.08441886	5.34652111	−1.51936235	5.72090302
Ec				
0.2	0.71273525	3.32236719	0.70433225	3.31630067
0.4	−0.60004878	4.67260633	−0.86649178	4.88900651
0.6	−2.01295066	6.12358149	−2.90133601	6.89687543
0.8	−3.54136725	7.69069921	−5.78374220	9.70455606
Pr				
0	2.00000000	2.00000000	2.00000000	2.00000000
0.01	1.94006341	2.06277512	1.94042744	2.06172087
0.5	−1.29309968	5.38461599	−1.80994558	5.82343923
1.0	−5.34596523	9.40302006	−11.9968129	16.1276131
Nb				
0.5	1.29523616	2.69306189	1.26097284	2.71387191
1.0	1.61827463	2.35452942	1.64442973	2.32856983
1.5	1.72579220	2.24016356	1.77183867	2.20247473
2.0	1.77959563	2.18188975	1.83518044	2.14101361
Nt				
0.2	−4.66844031	8.80042785	−5.66418623	9.74961998
0.4	−11.6651926	15.7189957	−13.5098551	17.9304355
0.6	−18.9882461	22.7426048	−21.5453643	26.5851065
0.8	−26.6345184	29.8585247	−29.7784418	35.7596799
Sc				
0.5	−1.32805779	5.41969422	−1.86178949	5.87447940
1.0	−1.29309968	5.38461599	−1.80994558	5.82343923
1.5	−1.25907661	5.35047139	−1.75997031	5.77423595
2.0	−1.22594700	5.31721870	−1.71174908	5.72675658
Sr				
0.5	−1.29309968	5.38461599	−1.80994558	5.82343923
1.0	−1.22594700	5.31721870	−1.71174908	5.72675658
1.5	−1.16221384	5.25323573	−1.62015815	5.63656647
2.0	−1.10161492	5.19238304	−1.53443576	5.55214398

with Λ_2, Sc, Sr whereas reversal effect is observed on the right plate for all values of Biot numbers as displayed in Table IV. For all the tables the values are chosen to be $Pr = 0.5$, $\Lambda_1 = \Lambda_2 = 5.0$, $Nt = Nb = 0.1$, $Ec = 0.5$, $Sc = 1.0$, $Sr = 0.5$, $R_T = 1$ except the varying parameter.

5. CONCLUSIONS

The problem of steady, laminar mixed convective flow in vertical duct filled with nanofluid is analyzed with the help of convective boundary conditions. The obtained equations were solved analytically using perturbation method which is applicable for values of perturbation parameter (i.e. Prandtl number) less than one and numerically by Runge-kutta method. The following were the observations made.

(a) The thermal Grashof number escaltes the velocity and temperature fields but it is not alter the concentration and naoparticle volume fraction. The mass Grashof number reduces the velocity at the left wall and enhance at the right wall and did not react on the concentration and naoparticle volume fraction.

(b) The Eckert number enhances the velocity and temperature were escalated whereas the concentration and nanoparticle volume fraction were declined. The response of Prandtl number was similar to that of Eckert number.

(c) As the Soret parameter enlarges the momentum, temperature, concentration and nanoparticle volume fraction were shrinked. The Schemidt parameter also show the similar properties as that of Soret parameter. The thermophoreis parameter augment the temperature whereas it depletes the concentration and nanoparticle volume fraction. The Brownian motion parameter acceleration parameter accelerates the concentration.

(d) The Nusselt values were supressed with the thermal and concentration Grashof numbers and was boosted with the remaining parameters at the cold plate. The reversal consequence was attained at the hot plate.

NOMENCLATURE

A	Constant [Pa m^{-1}]
Bi_1, Bi_2	Biot Numbers
Br	Brinkman number
Cp	Specific heat at constant pressure
C_f	Skin friction coefficient
C_0	Reference nanoparticle volume fraction
C	Dimensionless Nanoparticle volume fraction
C_1, C_2	Nanoparticle volume fraction at the wall
C^*	Nanoparticle volume fraction
D_B	Brownian diffusion coefficient (m^2/s)
D_T	Thermophoretic diffusion coefficient (m^2/s)
D_m	Mass diffusivity of the solute
$D(=2L)$	Hydraulic diameter [m]
Ec	Eckert number
f	Dimensionless steam function
g	Acceleration due to gravity [ms^{-2}]
GR_T	Grashof number ($g\beta\Delta TD^3/v^2$)
GR_ϕ	Solute Grashof number ($g\beta\Delta\phi D^3/v^2$)
h_1, h_2	Convective heat transfer coefficient [Wm^{-2}k^{-1}]
k	Thermal conductivity [Wm^{-1}k^{-1}]
L	Channel width [m]
n	Non-negative integer number
Nt	Thermopheresis parameter
Nb	Brownian motion parameter
Nu_1, Nu_2	Nusselt numbers
p	Pressure [Pa]
$P = p + \rho_0 gX$	Difference between the pressure and the hydrostatic pressure [Pa]
Pr	Prandtl number (v/α)
Re	Reynolds number (U_0D/ν)
R_T	Temperature difference ratio ($(T_2 - T_1)/\Delta T$)
S	Dimensionless parameter
Sc	Schmidt number
Sr	Soret number
Sh_1, Sh_2	Sherwood number
T	Temperature [K]
T_0	Reference temperature
T_1, T_2	Temperature at the hot fluid
T_∞	Ambient temperature
u	Dimensionless velocity in the X-direction
$u_n(y)$	Dimensionless functions
$\overline{u}$	Mean value of u
U	Velocity component in the X-direction [ms^{-1}]
U	Velocity [ms^{-1}]
U_0	Velocity
y	Dimensionless transverse coordinate
X	Stream wise coordinate [m]
Y	Transverse coordinate [m]

Greek Symbols

α	Thermal diffusivity ($K/\rho_0 c_0$) [m^{2}s^{-1}]
β_T	Thermal expansion coefficient [K^{-1}]
β_ϕ	Solutal volumetric coefficient
ΔT	Reference temperature
ΔC	Reference nanoparticle volume fraction
$\Delta\phi$	Reference concentration
τ_1, τ_2	Skin frictions
τ	Skin friction
ε	Dimensionless parameter
μ	Viscosity
θ	Dimensionless temperature
θ_b	Dimensionless bulk temperature
ϕ	Dimensionless concentration
ϕ^*	Concentration
ϕ_0^*	Reference concentration

ARTICLE

υ Kinematic viscosity of the base f (μ/ρ_0) $[m^2s^{-1}]$
Λ_1 Thermal Grashof number (GR_T/Re)
Λ_2 Mass Grashof number (GR_ϕ/Re)
μ Absolute viscosity of the base fluid
$(\rho c)_p$ Heat capacity of the nanoparticle material
$(\rho c)_f$ Heat capacity of the base fluid
ρ_0 Value of the mass density when $T = T_0$ $[Kgm^{-3}]$.

References and Notes

1. L. Godson, B. Raja, D. Mohan Lal, and S. Wongwises, *Renewable and Sustainable Energy Reviews* 14, 629 (**2010**).
2. H. Xie, Y. Wei, and C. Lifei, *NanoScale research Letters* 6, 124 (**2011**).
3. S. Choi, *ASME FED* 66, 99 (**1995**).
4. P.Keblinski, R. Prasher and J. Eapen, *J. Nanopart. Res.* 101089, 97 (**2008**).
5. Q. X. Wang and S. A. Mujumdar, *Braz. J. Chem. Engg*. 25, 613 (**2008**).
6. S. Kumar, S. K. Prasad, and J. Banerjee, *Appl. Math. Modeling* 34, 573 (**2010**).
7. H. Masuda, A. Ebata, K. Teramae, and N. Hishinuma, *Netsubussei* 7, 227 (**1993**).
8. J. Buongiorno and W. L. Hu, Nanofluid coolants for advanced nuclear power plants, *Proceedings of ICAPP '05* Paper No. 5705, Seoul (**2005**).
9. C. Kleinstreuer and Y. Feng, *Nanoscale Research Letters* 6, 1 (**2011**).
10. J. Buongiorno, *ASME J. Heat Transfer* 128, 240 (**2006**).
11. D. A. Nield and A. V. Kuznetsov, *Eur. J. Mech. B/Fluids* 29, 217 (**2010**).
12. D. A. Nield and A. V. Kuznetsov, *Eur. J. Mech. B/Fluids* 132, 052405 (**2010**).
13. J. Kim, C. K. Choi, T. Y. Kang and G. M. Kim, *Nanoscale Microscale Thermophys. Eng.* 10, 29 (**2006**).
14. J. Kim, C. K. Choi, and T. Y. Kang, *Int. J. Refrig.* 30, 323 (**2007**).
15. R. Savino and D. Paterna, *Phys. Fluids* 20, 017101 (**2008**).
16. S. Hazarika, S. Ahmed, and A. J. Chamkha, *Mathematics and Computers in Simulation* 93, 184 (**2020**).
17. S. Hazarika, S. Ahmed, and S. W. Yao, *Appl. Nanosci.* (**2021**), DOI: 10.1007/s13204-020-01655-w.
18. B. Goyeau, J. P. Songbe, and D. Gobin, *Int. J. Heat Mass Transfer* 39, 1363 (**1996**).
19. S. Ahmed, A. Batin, and A. J. Chamkha, *Int. J. of Num. Methods for Heat and Fluid Flow* 24, 1204 (**2014**).
20. S. Ahmed, O. A. Bég, and S. K. Ghosh, *Ain Shams Engng. J.* 5, 1249 (**2014**).
21. S. Ahmed, A. Batin, and A. J. Chamkha, *Alexandria Engng. J.* 54, 45 (**2014**).
22. M. Karimi-Fard, C. M.Charrier-Mojtabi, and K. Vafai, *Numer. Heat Transfer Part A* 30, 837 (**1997**).
23. P. Nithiarasu, T. Sundararajan, and N. K. Seetharamu, *Heat Mass Transfer* 24, 1121 (**1997**).
24. R. Bennacer, A. Tobbal, H. Beji, and P. Vasseur, *Int. J. Therm. Sci.* 40, 30 (**2001**).
25. A. M. Mansour, M. M. Abd-Elaziz, A. R. Mohamed, and E. S. Ahmed, *Transport in Porous Media* 87, 7 (**2011**).
26. M. A. Rashad, E. S. Ahmed, and M. A. Mansour, *Int. J. Numer. Methods Heat Fluid Flow* 24, 1124 (**2014**).
27. S. Ahmed, J. Zueco, and L. M. López-Ochoa, *Chem. Engng. Comm.* 201, 419 (**2014**).
28. J. C. Umavathi and Monica B. Mohite, *Heat Transfer Asian Research* 43, 628 (**2014**).
29. J. C. Umavathi, *Transport In Porous Media* 108, 659 (**2015**).
30. J. C. Umavathi and Marzio Sasso, Double diffusive convection in a porous medium layer saturated with an oldroyed nanofluid, *France Conference Proceedings AIP Publishers* (**2017**), pp. 0201661–02016610, DOI: 10.1063/1.4972758.
31. J. C. Umavathi, M. A. Sheremet, O. Ojjela, and G. Janardhan Reddy, *European J. B/Fluids* 65, 70 (**2017b**).
32. J. C. Umavathi and M. A. Sheremet, *Microfluidic Nanofluid* 21, 121 (**2017**).
33. J. Prathap Kumar, J. C. Umavathi and C. K. Murthy, *Int. J. Engng. Sci. and Research* 5, 11 (**2017**).
34. J. Zueco, S. Ahmed, and L. M. López-González, *Int. J. Heat and Mass Transfer* 110, 467 (**2017**).
35. A. Aziz, *Communications in Nonlinear Science and Numerical Simulation* 14, 1064 (**2009**).
36. A. Aziz, M. J. Uddin, M. A. A. Hamad, and A. I. M. Ismail, *Heat Transfer Asian Research* 41, 241 (**2012**).
37. O. D. Makinde, K. Zimba, and O. A. Beg, *International Journal of Thermal and Environmental Engineering* 4, 89 (**2012**).
38. R. Ahmad and W. A. Khan, *Heat Transfer Asian Research* 43, 17 (**2014**).
39. Wibulswas, Ph.D. thesis, London University, (**1966**).
40. R. W. Lyczkowski, C. W. Solbrig, and D. Gidaspow, Forced convective heat transfer in rectangular ducts general case of wall resistances and peripheral conduction, *Inst. of Gas Technol. Tech. Info. Center File* 3229 3424S, Chicago, Illonis (**1969**).
41. V. Javeri, *Warme Stoffubertragung* 9, 85 (**1976**).
42. E. Hicken, *Warme Stoffubertragung* 1, 98 (**1968**).
43. E. M. Sparrow and R. Siegel, *Int. J. Heat Mass Transfer* 1, 161 (**1960**).
44. V. Javeri, *Warme Stoffubertragung* 9, 85 (**1977**).
45. V. Javeri, *Int. J. Heat Mass Transfer* 10, 1029 (**1978**).
46. A. Barletta, *Int. J. Heat Mass Transfer* 41, 3501 (**1998**).
47. E. Zanchini, *Int. J. Heat Mass Transfer* 41, 3949 (**1998**).
48. N. C. Mahanthi and P. Gaur, *Journal of Applied Fluid Mechanics* 2, 23 (**2009**).
49. J. C. Umavathi and J. Sultana, *Int. J. Eng. Sci. Techno.* 3, 213 (**2011**).
50. J. C. Umavathi, A. J. Chamkha, and S. Veershetty, *Int. J. Energy and Technology* 4, 1 (**2012**).
51. J. C. Umavathi, J. Prathap Kumar, and J. Sultana, *Appl. Math. Mech.-Engl. Ed.* 33, 1015 (**2012**).
52. J. C. Umavathi, K. V. Prasad, and M. Shekar, *Int. J. Inno. Tech. Creat. Eng.* 2, 1 (**2012**).
53. J. C. Umavathi and Jaweriya Sultana, *J. Eng. Phys. and Thermo. Phys.* 85, 895 (**2012**).
54. J. C. Umavathi and Ali J. Chamkha, *Canadian Journal of Physics* 92, 1387 (**2014**).
55. J. Prathap Kumar, J. C. Umavathi, Ali J. Chamkha, and Y. Ramarao, *Canadian J. of Physics* 93, 698 (**2015**).
56. J. C. Umavathi and M. A. Sheremet, *European Journal of Mechanics B. Fluids* 55, 132 (**2016**).
57. J. Prathap Kumar, J. C. Umavathi, B. J. Gireesha, and M. Karuna Prasad, *J. of Nanofluids* 5, 1 (**2016**).
58. J. C. Umavathi, I. C. Liu, and M. A. Sheremet, *Heat Transfer Asian Research* 45, 661 (**2016**).
59. J. C. Umavathi, *J. Nanofluids* 6, 1 (**2017**).